BIOCHIMICA ET BIOPHYSICA ACTA

CONTENTS

BBA 99139

SPECTRAL ANALYSIS OF HIGH RESOLUTION DIRECT-DERIVATIVE MELTING CURVES OF DNA FOR INSTANTANEOUS AND TOTAL BASE COMPOSITION

R.D. BLAKE and STEPHEN G. LEFOLEY

Department of Biochemistry, University of Maine, Orono, Me. 04473 (U.S.A.)

(Received July 19th, 1977)

Summary

Derivative melting profiles of DNA have been obtained directly by recording the difference in absorbance between two identical solutions maintained at a small constant temperature differential. This ΔA is monitored continuously with increasing temperature in a ratio recording spectrophotometer. Resolution of complex hyperfine structure in the profiles of small homogeneous viral DNAs appears to be significantly better than has been produced by various numerical methods of differentiation.

In addition, a spectral method has been modified that permits easy analysis for DNA base composition from the ratio of derivative melting curves obtained at 282 and 260 nm. Eight bacterial and three vertebrate DNAs have been analyzed for total base composition from the product of the instantaneous base composition at small temperature intervals (0.05°C) throughout the entire melting region and the integrated area of the 282 nm profile. The results are in excellent agreement with values determined by traditional methods.

Introduction

The apparent sensitivity of optical melting curves of DNA has improved dramatically over the past few years, facilitating the numerical differentiation of absorbances from observed profiles (refs. e.g. 1—6). The technique of differentiation to enhance fine structure is well known; making complex profiles more amenable to analysis. We shall describe some analyses of melting curves obtained by the simpler alternative of recording the derivative of the absorbance change directly between two identical solutions maintained at a small constant temperature differential. Comparisons of the derivative melting profiles obtained in this fashion indicates the resolution of hyperfine structure in the melting profiles of comparatively small homogeneous DNAs, such as λ

234

or PM2 DNA, to be no less than, and in many respects much higher than those obtained by numerical differentiation.

High resolution melting profiles of DNA represent thermodynamical maps of regions smaller than 0.5% of the total genome. If the DNA is sufficiently short, melting exhibits a fine structure arising from specific subtransitions [6], and under favorable conditions may reflect the base composition over regions as small as 300 base pairs [4]. However, such profiles raise questions of the suitability of analyses derived from the familiar macroscopic linear free energy expression for the dependence of melting temperature, T_m, on G + C composition [7]. The analysis of particular subtransitions for the number of base pairs, or the instantaneous base composition, or the variability of the latter under a resolved band are matters of considerable interest; therefore, we have refined a spectral method that can be used to quantitate both instantaneous and total base composition under any DNA derivative melting profile.

Materials and Methods

DNA. DNAs from PM2, $\lambda(CI_{5\text{-}5}S_7)$, T4, *Escherichia coli, Bacillus subtilis,* Ps. BAL 31, calf thymus, salmon sperm and moose liver (*Alces alces*) were isolated according to established procedures [8—10]. In addition, DNAs from *Clostridium perfringens, Pseudomonas fluorescence,* T4, *B. subtilis, E. coli, Micrococcus lysodeikticus,* calf thymus, salmon sperm, and synthetic poly(dA · dT), poly(dA · dT), poly[d(A-T) · d(A-T)] and poly[d(G-A) · d(T-C)] were purchased. No differences could be discerned in the high resolution melting profiles of DNAs from the same species but from different sources or prepared by different methods; though some commercial DNAs required further deproteinization by phenol.

The mean size and size distribution of all DNAs were examined by electrophoresis through 0.5% agarose on 0.75 mm X 12 cm vertical slab gel. All runs were framed by DNAs of predefined size and mobilities determined from fluorescence-microdensitometer tracings. Size standards included monodisperse preparations of sheared calf thymus DNA, λ, PM2 and the six ECO RI endonuclease products of λ [11]. It was observed that the size of most prokaryotic DNAs exceeded the upper resolving limit of the gel (approx. $30 \cdot 10^6$ daltons). However, the vertebrate DNAs exhibited some detectable skewing toward lower molecular weights, which, nevertheless, exceeded $20 \cdot 10^6$.

Solvent. The solvent in all cases consisted of 7.5 mM NaCl, 5 mM sodium cacodylate, 0.2 mM Na-EDTA, pH 6.85 ([Na$^+$] = 0.012 M). The precise Na$^+$ concentration was confirmed by the temperature at the inflection point in melting curves of poly(rA · rU) (38.76 ± 18°C) [12] and poly(dA · dT) (48.60 ± 0.18°C) [13]. A small amount of poly(dA · dT) ($A_{260nm} \approx 0.10$) was added to all DNAs to provide a distinguishable marker in the derivative profiles. The poly(dA · dT) profile is sensitive to variations in the Na$^+$ concentration of less than 1%, or ±0.1 mM.

Direct-derivative melting curves. Melting of DNA was monitored by the loss of hypochomicity at selected wavelengths in the form of a derivative $dA(\lambda,nm)/dT^*$. In a manner similar in principle to that described by Römer et al. [14],

derivative p
absorbance.
different te
Cary 118C,
··· ? maxi-
ie limit of
·ni instabil
selected t
involved so:
calibration
arc, and cl
absolute a
depending
microcells r
from evapo
always <0.
expansion w
The temp
circulating
·ter was
perature
1.0°C/n
reduction; ;
regulators c
from the H
laboratory.)
through a
thoroughly
differential
97°C range
monitored
Yellow Spri
the cells an
The te
ples. Th
perature
latinum re
The 500 Ω
25 mm wer
amplificatio
routinely cl
nucleotide
cerned in th

Results

Direct deriv.
it is cont

than those

al maps of
ntly short,
s [6]. and
regions as
ons of the
free energy
C composi-
base pairs,
ter under a
e refined a
s and total

subtilis, Ps.
ere isolated
NAs from
lis, E. co.,
poly(dA ·
T-C)] were
on melting
or prepared
ther depro-

by electro-
el. All runs
ained from
ied mono-
six ECO RI
ze of most
el (approx.
detectable
ceeded 20 ·

nM sodium
precise Na⁺
on point in
T) (48.60 ±
as added to
ofiles. The
tion of less

by the loss
$dA(\lambda,nm)/$
et al. [14],

derivative profiles were obtained directly by measuring the small difference in absorbance, ΔA (λ), between two identical solutions maintained at slightly different temperatures, ΔT^*. This ΔA (λ) was monitored continuously in a Cary 118C, a ratio recording spectrophotometer with double monochromater, and a maximum noise level of less than 0.0003 A in the derivative curves, fixing the limit of resolution at that level. Occasional fluctuations caused by the normal instability of the deuterium arc (± 0.0003 A) could be eliminated by using a selected tungsten-halogen lamp with clean quartz envelope; which, of course, involved some sacrifice of intensity in the far ultraviolet region. Wavelength calibration was established with the emission lines of a high pressure mercury arc, and checked occasionally with the spectrum of benzene vapor. The absolute absorbances of samples varied between 0.10 and 1.5 A_{260nm} depending upon the sample, the desired sensitivity and ΔT^*. Teflon stoppered microcells requiring 500 μl of sample were normally used; with negligible losses from evaporation. Since the difference in temperature between samples was always <0.5°C, no correction of absorbance due to dilution from thermal expansion was deemed necessary.

The temperatures of the two samples were controlled independently by circulating water through a pair of custom-made baffled sample chambers. This water was thermoregulated with a pair of modified Haake-FS baths. The temperature was increased linearly at discrete, reproducible rates between 0.10 and 1.0°C/min with a pair of stepper motors (12 V DC, 0.05° step angle, 150X reduction; available from Hurst Mfg. Co.) connected directly to the thermoregulators of the Haake baths. (Pulse and driver circuit boards are available from the Hurst Co. The 12 V power supply was built by W. Yen of this laboratory.) Fine adjustment of the duty cycle of the bath heaters was made through a ten-turn potentiometer on the voltage switching circuit. By thoroughly insulating the baths, circulating tubes and sample chambers, a differential between the two samples as small as 0.15 = 0.02°C over the 20—97°C range of all experiments could be maintained. Temperatures were monitored to a hundredth of a degree with a pair of thermistors (Type 721, Yellow Springs Inst. Co.), calibrated to within 0.1°C of absolute, mounted in the cells and connected to a suitable bridge and 4½ digit DVM with BCD output. The temperature scale of all experiments represents the mean between samples. The ability of this system to maintain a constant ΔT^* over a wide temperature range was monitored continuously with a linearized, differential platinum resistance bulb transmitter (Moore Industries) and 4½ digit DVM. The 500 Ω Pt elements (0°C, YSI-Sostman) measuring 2 mm diameter by 25 mm were mounted in dummy cells in tandem with the sample cells. Signal amplification was approx. 1 V/1°C difference. Constancy of ΔT^* was also routinely checked by melting a mixture of five synthetic homo- and copolynucleotide helices at $\Delta T^* = 0$. No significant deviation or drift was ever discerned in these tests.

Results

Direct derivative curves

It is convenient to classify melting profiles into three basic types according

to the size and sequence homogeneity of the DNA. To demonstrate the resolving capability of the direct method, examples of all thre classes are illustrated. First, are the polyphasic melting of short, homogeneous viral DNAs consisting of unique sequences. The example of $\lambda(CI_{875}S_7)$ DNA is illustrated in Fig. 1. Even when recorded for analytical purposes at over 5-fold greater sensitivity (Figs. 1b—1d), these curves are reproducible almost to within the noise level ($\pm 0.0001 A$). The profile obtained for λ DNA is in good but not altogether quantitative agreement with published high resolution profiles obtained by numerical differentiation. The numbered identification of subtransitional bands corresponds quite well to that of Yabuki et al. [1,2] for the same temperature sensitive $CI_{875}S_7$ strain; while lettered numbers indicate the occurrence of additional bands either unresolved or non-existence in the previous work. Until a direct comparison on the same DNA sample can be made, however, any differences that might be detected should probably not be construed as originating from our different techniques.

The melting of λ DNA involves a minimum of 24 discrete subtransitions, each occurring over a range of approx. 0.4°C; plus another four to six that occur within 0.2°C of one of the major subtransitions and so are perceived only as shoulders. A detailed analysis of the high resolution profiles of λ and open PM2 DNAs (Blake, Stephens and Yen, unpublished) indicates that during the earliest stages of melting each subtransition represents the dissociation of a block of base pairs to form a local bubble in the DNA. Later subtransitions include the dissociation of segments between loops and therefore are associated with rather abrupt increases of loop entropy, followed by a cascading collapse of nearby segments.

The second type of curve is represented by those obtained with bacterial and large viral DNAs of molecular weight greater than say $150 \cdot 10^6$ and possessing essentially unique sequences. Such DNAs exhibit comparatively smooth, mono-

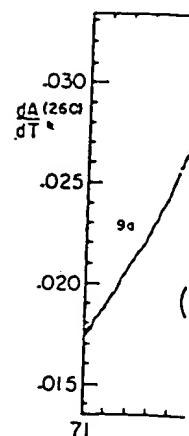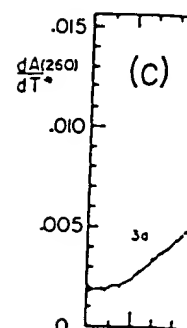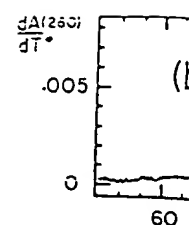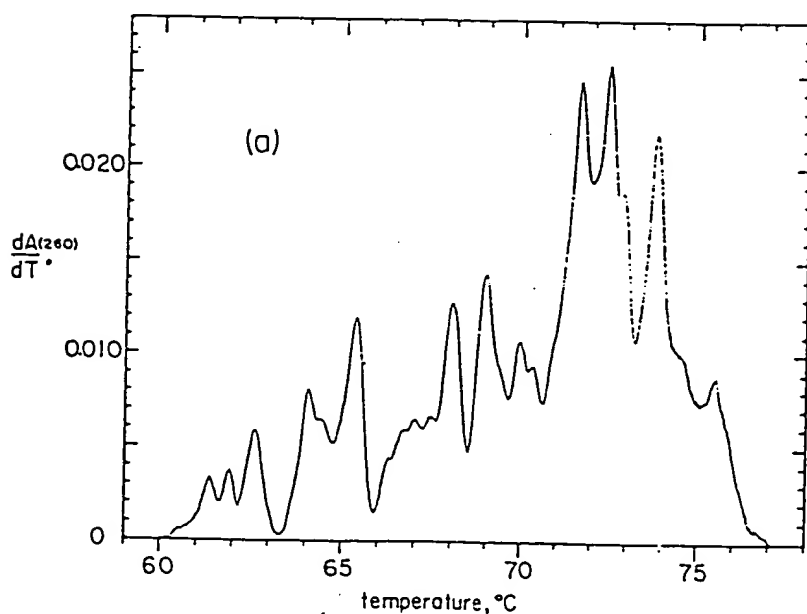

1. Direct-deriv:
These experimer
plot of the comple:
of 0.015°C and con
tion given in Table
melting at greater s
the spectrophotom.
(with automatic ad
increasing temperat

phasic profiles
Fig. 2.

We expect t
λ DNA, to in
reduction in tl

ate the
ses are
l DNAs
ated in
greater
in the
out not
profiles
of sub-
for the
ndicate
e in the
can be
not be

sitions,
six that
ed only
d open
ring the
on of a
nsitions
ociated
collapse

rial and
ssessing
mono-
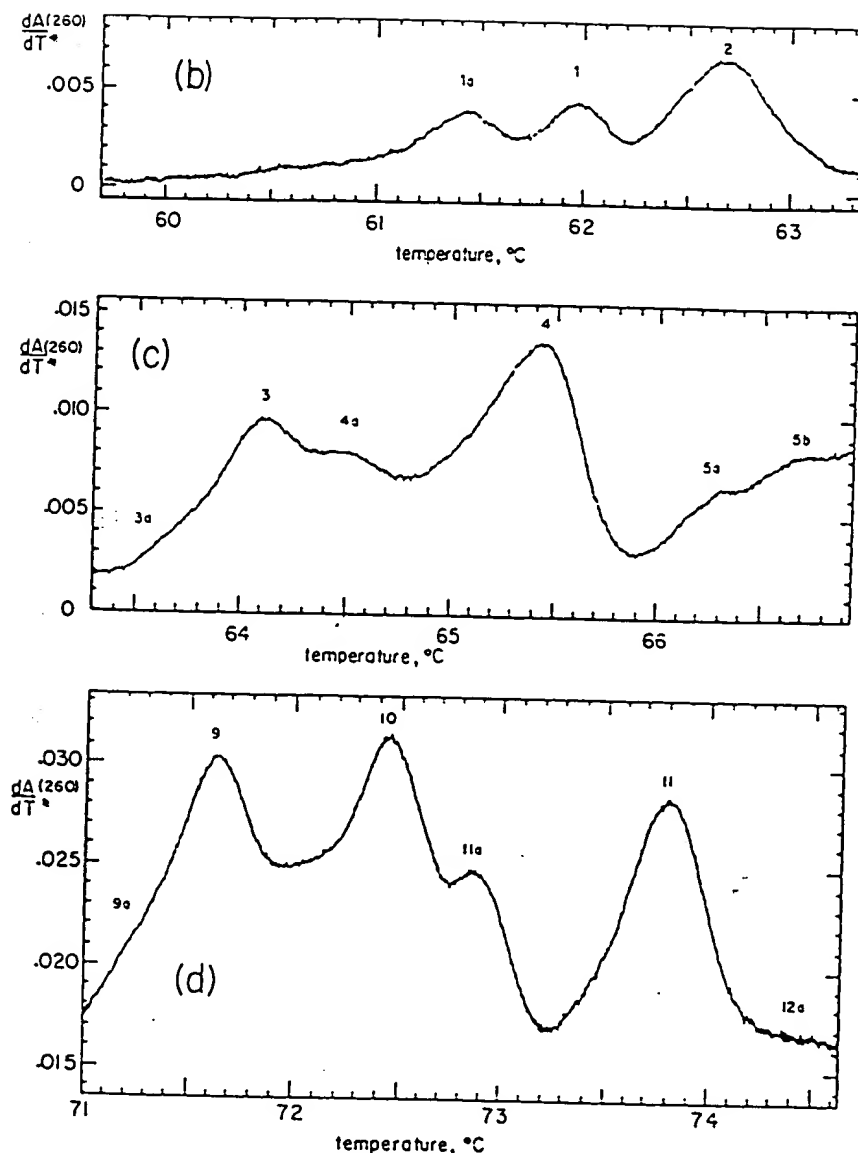
Fig. 1. Direct-derivative melting curves of $\lambda CI_{857}S_7$ DNA obtained at 260 nm at a linear rate of 6.62°C/n. These experiments were conducted in the standard buffer, $[Na^+] = 0.0120$ M. (a) Computer graphics plot of the complete profile. This plot was produced with derivative absorbance data gathered at intervals of 0.015°C and corrected for a slight drift in the baseline; and used also for calculations of G + C composition given in Table I. Conditions: $\Delta T^\circ = 0.263°C$, $A_{260nm} = 1.480$. (b—d) These figures show sections of melting at greater sensitivity over narrow temperature regions. Data directly from the analog recorder on the spectrophotometer were photocopied. Conditions: $\Delta T^\circ = 0.224°C$, $A_{260nm} = 1.704$, slit = 0.80 mm (with automatic adjustment of the phototube gain to compensate for the increase in absorbance with increasing temperature).

phasic profiles. The example of the melting of *B. subtilis* DNA is illustrated in Fig. 2.

We expect the number of unique subtransitions, so distinct in the melting of λ DNA, to increase with DNA length. The eventual consequence will be a reduction in the polyphasic resolution of a profile that more resembles a nor-

238

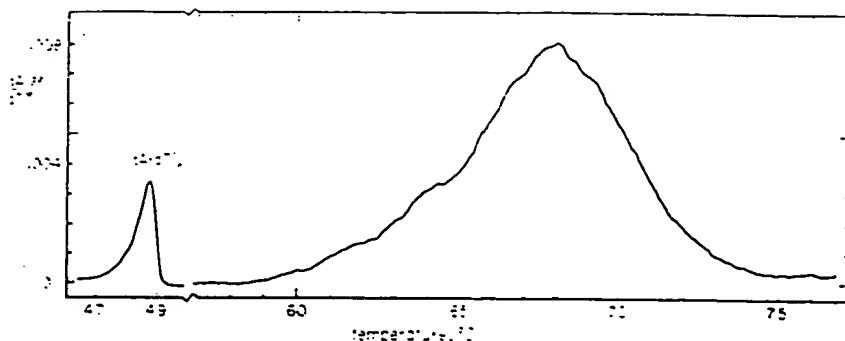Fig. 2. Melting curve of *B. subtilis* DNA recorded at 260 nm at a linear rate of 12.86°C/h. Conditions: $\Delta T^* = 0.360°C$, $A_{260nm} = 0.5521$. The spike at lower temperature was produced by poly(dA · dT) that was added to the *B. subtilis* DNA. The region in between was cut out, condensing the figure to more reasonable proportions, yet it can be seen that the baseline remained constant within 0.0001 A throughout the entire experiment.

mal distribution of a large number of closely overlapping subtransitions. This is what is observed. At 10—100 times the length of λ DNA the melting profiles of bacterial and larger viral DNAs lose resolution between individual sub-transitions, though a trace of fine structure often persists in the early stages. This irregularity in an otherwise smooth profile is quite reproducible, and is clearly evident in the *B. subtilis* curve of Fig. 2, and probably reflects the more extreme non-random distribution of (A + T)-rich segments which melt early.

The third type of profile is produced by DNAs from higher eukaryotes, and is represented here (Fig. 3) by the profile for calf thymus DNA. Members of this third class generally melt over a wider temperature range and are poly-phasic. We count four distinct peaks and at least three shoulders in the calf
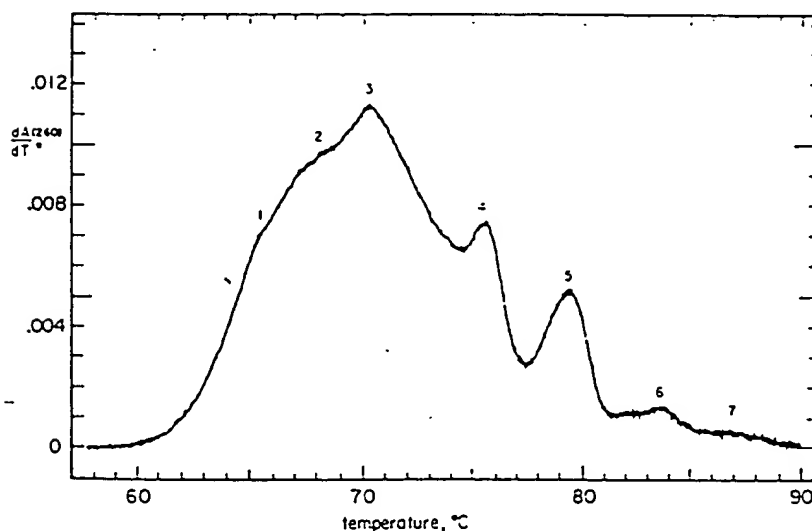

Fig. 3. The melting of calf thymus DNA recorded at 260 nm at a linear rate of 12.86°C/h. Conditions: $\Delta T^* = 0.32°C$, $A_{260nm} = 0.772$.

thymus profile. Slightly higher resolution profiles obtained recently (not shown) reveal a fifth peak between Nos. 3 and 4 in Fig. 3. These bands are not subtransitional processes. Calf DNA is almost 60 000 times longer than λ DNA and is therefore most unlikely to exhibit any subtransitional detail. Moreover, the bands seen in the calf DNA profile occur over 3—4°C, approximately ten times the breadth of individual subtransitions. We suspect these bands represent the magnified effects of repetitive sequences superimposed on a broad background of unique sequences. One difficulty with this hypothesis, however, is that melting profiles of DNAs from related eukaryotic species are quite different [15], while the overall base composition remains about the same. This raises interesting questions about the origin and preservation of such bands as putative repetitive sequences, since the range of base composition under any one band is obviously quite narrow. If indeed they are repetitive sequences, they have either evolved quite abruptly and/or are replicated in some special, interdependent fashion so that evolutionary changes in base composition are preserved in all copies of a repeated sequence.

Spectral dispersion of derivative melting curves

Analytical considerations. Felsenfeld and Fresco and their respective co-workers [16—18] pioneered the spectral approach for the determination of base composition from melting curves. Its applicability to derivative profiles has been demonstrated [14,19—21], however, a rigorous quantitative analysis for base composition with special emphasis on high resolution derivative profiles has not been developed. The basis of this approach is a dispersion of the hypochromic effect with wavelength, λ. Changes in absorption can be resolved into components arising from $A \cdot T$ and $G \cdot C$ base pairs:

$$\Delta A_{obs}(\lambda) = \Delta A_{a \cdot t}(\lambda) + \Delta A_{g \cdot c}(\lambda) \tag{1}$$

where ΔA_{obs} is the increase observed and $\Delta A_{a \cdot t}$ and $\Delta A_{g \cdot c}$ are components of that change arising from the dissociation of $A \cdot T$ and $G \cdot C$ base pairs. From the Beer-Lambert Law,

$$\Delta A_{a \cdot t}(\lambda) = \Delta C_{a \cdot t} \cdot \Delta \epsilon_{a \cdot t}(\lambda) \tag{2}$$

(and similarly for $\Delta A_{g \cdot c}(\lambda)$), where $\Delta C_{a \cdot t}$ is the decrease in the concentration of $A \cdot T$ base pairs over the temperature interval of ΔA_{obs} and $\Delta \epsilon_{a \cdot t}$ is the corresponding change in extinction coefficient of an $A \cdot T$ base pair at wavelength, λ. The instantaneous mol fraction of $G \cdot C$ base pairs, $f_{g \cdot c}$, corresponding to the change in absorption is given by

$$f_{g \cdot c} = \frac{\Delta C_{g \cdot c}}{\Delta C_{a \cdot t} + \Delta C_{g \cdot c}} = \frac{\Delta A_{g \cdot c}(\lambda)}{\Delta A_{a \cdot t}(\lambda) + \Delta A_{g \cdot c}(\lambda)} \tag{3}$$

Short of a complete spectral analysis [16—18] adequate precision can be achieved simply by taking the ratio of two melting curves obtained at wavelengths where the contribution of $A \cdot T$ and $G \cdot C$ base pairs to ΔA_{obs} show the greatest difference. Allowing consideration for further simplification, it is most convenient if one wavelength, λ_1, is isosbestic for $A \cdot T$ base pairs, so that $\Delta A_{a \cdot t}(\lambda_1)/\Delta A_{a \cdot t}(\lambda_2) = 0$. For maximum sensitivity the other wavelength, λ_2, is then chosen that gives the largest absorbance change in difference spectra for

the dissociation of an $A \cdot T$ base pair. The isosbestic wavelength for the $A \cdot T$ base pair is popularly believed to be at 280 nm, however, we find that wavelength to be isosbestic only for the alternating $d(A-T) \cdot d(A-T)$ copolymer. Fig. 4 illustrates melting curves for a 1 : 1 mixture of $d(A-T) \cdot d(A \cdot T)$ and $dA \cdot dT$ at four wavelengths. We see that 280 nm is isosbestic for $d(A-T) \cdot d(A-T)$ while that for $dA \cdot dT$ is beyond 284 nm, demonstrating a dependence of the absorption between 280 and 284 nm on three out of the seven possible A-T nearest neighbors in DNA, with the sum of their absorbances being isosbestic at (or very close to) 282 nm. Similar profiles of $d(A-C) \cdot d(G-T)$ indicate an isosbestic wavelength also rather near 282 nm for the sum of $\left\langle \begin{array}{c} A \cdot T \\ C \cdot G \end{array} \right\rangle$ and $\left\langle \begin{array}{c} C \cdot G \\ A \cdot T \end{array} \right\rangle$ nearest neighbors. On the basis of these results and presuming the $A \cdot T$ base pair in DNA to have a more-or-less random distribution of all seven nearest neighbors we are persuaded that the minimum absorbance change for the dissociation of the $A \cdot T$ base pair will occur at (or very near) 282 nm.

The largest at close to 260 nm, obtain

$i_{g \cdot c} = \Delta \epsilon_{a \cdot t} (260$

relating the rati 260.0 nm at any instant. From it $dA \cdot dT$ at 260 n $mol^{-1} \cdot cm^{-1}$ for 2765 ± 95 l · mol evaluated in Eqn.

Variation of T_m
A convenient sponding to the (upper plateau) mate a linear de] refs. 7, 22—24), DNAs from diffe attempted to concentration or DNAs simultane(*E. coli* ($F_{g \cdot c} = 0$. as well as in cor Table I represent amount of $dA \cdot$ Fig. 2), since its fluctuations in [tion of T_m with sion fitting the d

$F_{g \cdot c} = 0.0199 \ T_n$

correlation ression for a ear expression

$F_{g \cdot c} = -0.5701 -$

describing the l reason to constr indicate the de] [26]. Although we nevertheless

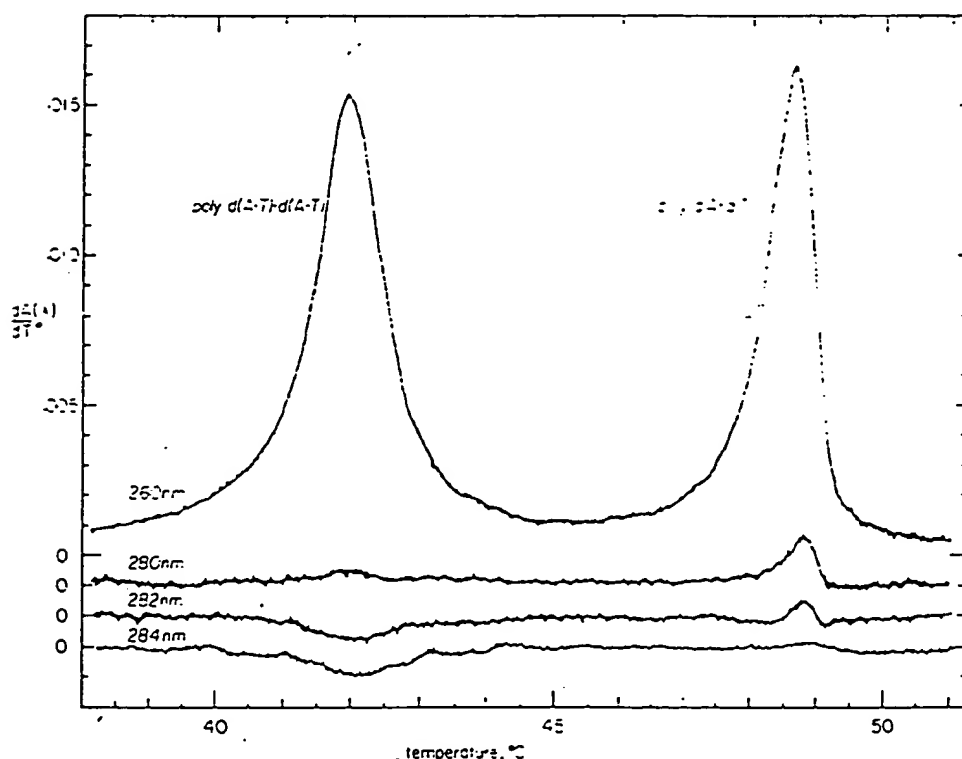*Variation of Δ $i_{g \cdot c}$*
The two rem

Fig. 4. The melting of a 1.2 : 1 mixture of poly[d(A-T) · d(T-A)] and poly(dA · dT) at four wavelengths: 260 nm, where the increase in absorbance on melting is maximal; 280 nm, where the change is approximately zero for d(A-T) · d(T-A), i.e. the absorbances of helically stacked and disordered A · T base pairs are identical (isosbestic), while dA · dT still shows a significant increase in absorbance on melting; 282 nm, where the decrease in absorbance on melting d(A-T) · d(T-A) is almost equivalent to the increase for dA · dT; and 284 nm, where the decrease for d(A-T) · d(T-A) is only slightly larger, while the change for dA · dT is almost zero. Poly(dA · dT) shows a rather diffuse approach to an isosbestic wavelength between 284 and 287 nm for the order ⇌ disorder transition of the helix. The precise isosbestic point appears close to 286 nm. Conditions: $\Delta T^{\bullet} = 0.224°C$, $\Delta A_{260nm} = 0.4063$.

The largest absorbance change for the dissociation of an $A \cdot T$ base pair is close to 260 nm. Thus, given that ΔT^* is identical for both melting curves we obtain

$$f_{g \cdot c} = \Delta\epsilon_{a \cdot t}(260 \text{ nm}) \left/ \frac{\Delta\epsilon_{g \cdot c}(282 \text{ nm})}{\Delta A_{282\text{nm}}/\Delta A_{260\text{nm}}} - [\Delta\epsilon_{g \cdot c}(260 \text{ nm}) - \Delta\epsilon_{a \cdot t}(260 \text{ nm})] \right.$$

(4)

relating the ratio of derivative melting curves obtained at 282.0 nm and 260.0 nm at any temperature to the $G \cdot C$ base composition dissociating at that instant. From integration of several melting curves of $d(A\text{-}T) \cdot d(A\text{-}T)$ and $dA \cdot dT$ at 260 nm (cf. Fig. 4) and an average extinction coefficient of 9737 $l \cdot$ mol$^{-1} \cdot$ cm^{-1} for the dissociated $A \cdot T$ base pair we find that $\Delta\epsilon_{a \cdot t}$ (260 nm) = 2765 ± 95 $l \cdot$ mol$^{-1} \cdot$ cm^{-1}. Consequently, just two constants remain to be evaluated in Eqn. 4.

Variation of T_m with total $G + C$ composition, $F_{g \cdot c}$

A convenient measure of base composition is the temperature, T_m, corresponding to the midpoint in the integrated melting curves, $A(T_m) = 0.5 [A$ (upper plateau) $- A$ (lower)]. The T_m has been shown repeatedly to approximate a linear dependence on total $G + C$ content, $(\partial T_m / \partial F_{g \cdot c})_M \cdot = 50°C$, (e.g. refs. 7, 22—24), where the accessible range is limited to $0.72 > F_{g \cdot c} > 0.27$ for DNAs from different organisms. In establishing a standard curve for this study, we attempted to minimize random errors caused by small fluctuations in cation concentration or temperature by melting two, and occasionally three different DNAs simultaneously. For example, DNAs from Cl. perfringens ($F_{g \cdot c} = 0.30$), E. coli ($F_{g \cdot c} = 0.507$) and M. lysodeikticus ($F_{g \cdot c} = 0.72$) were melted together as well as in combination with other standard DNAs. The T_m results given in Table I represent averages of at least five measurements on each DNA. A tiny amount of $dA \cdot dT$ ($A_{260\text{nm}} \approx 0.10$) was always added to each sample (cf. Fig. 2), since its profile serves as an especially sensitive indicator of slight fluctuations in [Na$^+$] or temperature. The filled circles in Fig. 5 show the variation of T_m with $F_{g \cdot c}$ for eight standard DNAs. The linear least squares expression fitting the data in this figure is given by

$$F_{g \cdot c} = 0.0199 \, T_m - 0.990$$

(5)

with correlation coefficient of 0.998. We find, however, that the variance about regression for a second degree polynomial is less than half that for the simple linear expression. The data are better fit by

$$F_{g \cdot c} = -0.5701 + 0.0100 \cdot T_m + 7.1525 \times 10^{-5} \, T_m^2$$

(6)

describing the line through data in Fig. 5. There is no rigorous theoretical reason to constrain these data to a linear form; on the contrary, recent studies indicate the dependence of T_m on $F_{g \cdot c}$ may approximate a cubic polynomial [26]. Although the variance is improved slightly (by 10%) for a cubic equation, we nevertheless use Eqn. 6 for subsequent analysis.

Variation of $\Delta A_{282\text{nm}}/\Delta A_{260\text{nm}}$ with the Instantaneous $G + C$ composition, $f_{g \cdot c}$

The two remaining constants in Eqn. 4, $\Delta\epsilon_{g \cdot c}$ (282 nm) and $\Delta\epsilon_{g \cdot c}$ (260 nm),

TABLE I

BASE COMPOSITIONS OF SELECTED DNAs DETERMINED BY THERMAL AND SPECTRAL METHODS

DNA	T_m (°C) *	Base composition (mol fraction of G · C base pairs)				
		Instantaneous $f_{g·c}$ at T_m		Total $F_{g·c}$ (Eqn. 7)		Total $F_{g·c}$
		Thermal (Eqn. 6)	Spectral (Eqn. 4)	Thermal	Spectral	from the literature [25]
C. perfringens	59.66	0.278	0.310	0.277	0.313	0.299
Pseudomonas BAL 31	66.25	0.413	0.412	0.412	0.419	—
B. subtilis	67.88	0.436	0.410	0.434	0.387	0.424
Poly[d(A-C) · d(G-T)]	71.24	0.502	0.489	**	**	(0.500)
λCI857S7	71.42	0.507	0.559	0.490	0.490	0.490
E. coli	71.69	0.512	0.507	0.513	0.496	0.507
Ps. fluorescens	76.69	0.614	0.627	0.619	0.606	0.620
M. lysodeikticus	80.76	0.699	0.739	0.697	0.676	0.720
Calf thymus	67.95	0.438	0.419	0.449	0.432	0.431
Moose liver (A. alces)	68.70	0.452	0.437	0.447	0.452	—
Salmon sperm	68.75	0.453	0.435	0.457	0.432	0.423
Average	±0.26°C	±3.0%	±3.6%	±1.9%	±3.8%	±2.9%

* Solvent: 0.0075 M NaCl, 0.005 M sodium cacodylate, 0.0002 M Na-EDTA, pH 6.85 ([Na⁺] = 0.012 M).

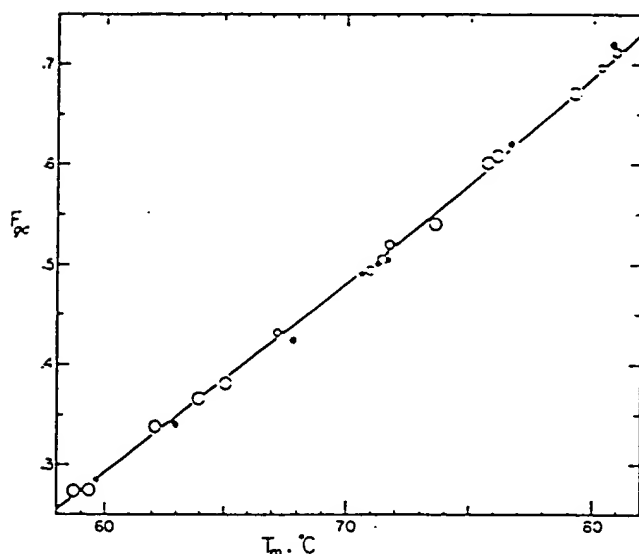** An analysis of melting is in progress (cf. refs. 29 and 30).

Fig. 5. Variation of T_m with $F_{g·c}$. The filled circles (•) represent the average of at least five measurements of T_m on Cl. perfringens, T4, B. subtilis, λ, poly[d(A-C) · d(G-T)], E. coli, Ps. fluorescens, and M. lysodeikticus DNA. Numerical values for T_m and $F_{g·c}$ are given in columns 2 and 7 of Table I. Standard deviations, reflected in the diameter of each point, are given only for the scatter in T_m and not for $F_{g·c}$. Open circles (O) represent data from Mandel et al. [24]. These latter data were obtained at slightly higher [Na⁺], and so required a correction of about 4°C according to the expression of Owen et al. [23] (cf. Frank-Kamenetskii) [25], modified slightly according to our own determination of the dependence of T_m on both $F_{g·c}$ and [Na⁺]. The line through data is given by Eqn. 6.

were evaluated
with standard I
the latter were
the results of t
overlapping, co
range of base
represent the c
meaningful segn
smallest length

Evaluation of
Eqn. 4 to the d
$\Delta\epsilon_{g·c}$ (282 nm)
calculate the in
Table I. Agreem-
course, we expe
the spectral Eqr
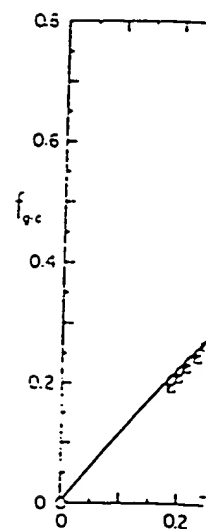the level of pre
add that the rel
between 0.2 and
Since 282.0 n

Fig. 6. Variation of
ΔA_{260nm} with $f_{g·c}$
melting curves of Cl.
E. coli (△), Ps. fluor
where $f_{g·c} = 2.765/($
mined at 0.05°C intu
pair of profiles, and
upper and lower lim
fore are intrinsically
by fine adjustment
was obtained by care

were evaluated empirically from the variation of $\Delta A_{282nm}/\Delta A_{260nm}$, obtained with standard DNAs, with the instantaneous base composition, $f_{g \cdot c}$. Values for the latter were obtained by interpolating results in Fig. 5 with Eqn. 6. When the results of triplicate analysis on six bacterial DNAs are plotted (Fig. 6) an overlapping, continuous function is obtained that extends beyond the usual range of base composition, $0.76 > f_{g \cdot c} > 0.18$. Presumably these boundaries represent the compositional extremes that can be found in any biologically meaningful segment of 200–400 base pairs, since that length appears to be the smallest length producing an observable subtransition [3–5].

Evaluation of $\Delta\epsilon_{g \cdot c}$ (260 nm) and $\Delta\epsilon_{g \cdot c}$ (282 nm) was by least squares fit of Eqn. 4 to the data in Fig. 6. We find that $\Delta\epsilon_{g \cdot c}$ (260 nm) = 1014 ± 138, while $\Delta\epsilon_{g \cdot c}$ (282 nm) = 2009 ± 106 l·mol^{-1}·cm^{-1} (solid line). When used to calculate the instantaneous $f_{g \cdot c}$ at T_m, Eqn. 4 gave the results in column 4 of Table I. Agreement with those calculated by Eqn. 6, is generally within ±3%. Of course, we expect a good agreement since Eqn. 6 was used as standard in fitting the spectral Eqn. 4 in the first place. The comparison is made here just to show the level of precision that can be achieved by the spectral method. We might add that the relationship of the spectral equation is independent of ΔT^* used between 0.2 and 2.0°C.

Since 282.0 nm is isosbestic for the A · T base pair, the fraction of G · C base
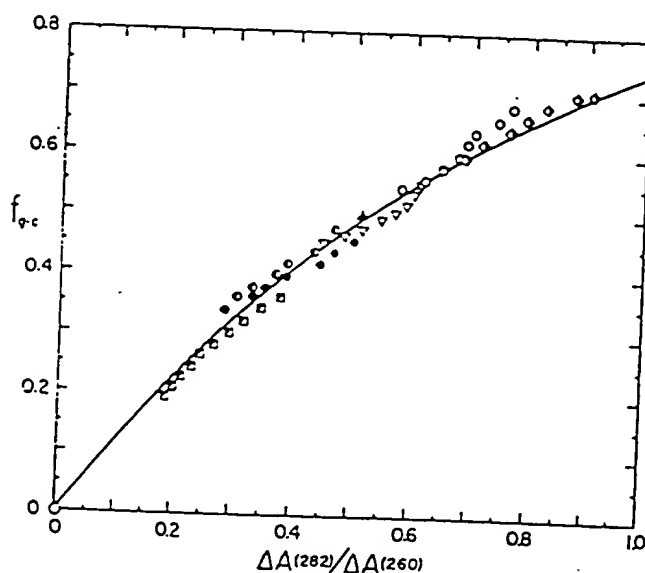

Fig. 6. Variation of the ratio of the melting curve obtained at 282 nm to that at 260 nm, $\Delta A_{282nm}/\Delta A_{260nm}$, with $f_{g \cdot c}$, the fractional G + C composition dissociating at that temperature. Data are from the melting curves of Cl. perfringens (□), Pseudomonas BAL 31 (●), B. subtilis (◇), poly[d(A-C) · d(G-T)] (▲), E. coli (△), Ps. fluorescens (○) and M. lysodeikticus (◇). The line through data is given by expression 4, where $f_{g \cdot c} = 2.765/[(2.009/\Delta A_{282nm}/\Delta A_{260nm}) - 1.752]$. The $\Delta A_{282nm}/\Delta A_{260nm}$ ratio was determined at 0.05°C intervals over the complete temperature range of observable melting in each wavelength pair of profiles, and limited here to every 20th point and central 95–98% of each profile. The extreme upper and lower limits of melting represent $\Delta A_{282nm}/\Delta A_{260nm}$ ratios of very small numbers and therefore are intrinsically less accurate, although total modulation of scatter at the extremes could be achieved by fine adjustment of the baseline (rarely more than ±0.0001 A) and/or curve smoothing. The baseline was obtained by careful extrapolation into the melting region from well above and below it.

244
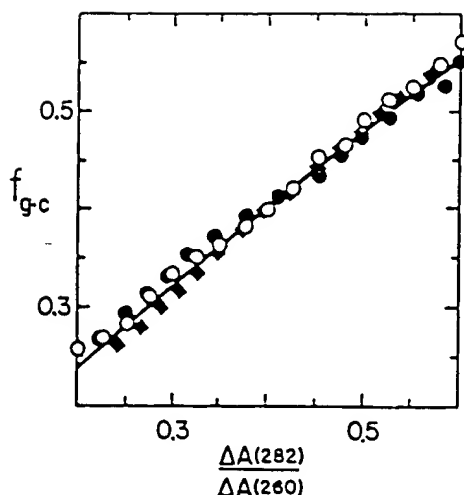
Fig. 7. Variation of $\Delta A_{282nm}/\Delta A_{260nm}$ with $f_{g\cdot c}$ for DNAs from calf thymus (•), salmon sperm (○) and moose liver (♦).

pairs dissociating under any subtransitional band, or total fraction under an entire profile will be proportional to the integrated area under the derivative profile between the extreme upper and lower limits of melting, T_1 and T_2:

$$F_{g\cdot c} = \sum_{T_1}^{T_2} \frac{\Delta A_{282nm}(T)}{\sum_{T_1}^{T_2} \Delta A_{282nm}} \cdot f_{g\cdot c}(T) \qquad (7)$$

Base compositions determined in this fashion are given in Table I for both thermodynamic (column 5) and spectral $f_{g\cdot c}$ (column 6). The apparent precision of the spectral method for the determination of total base composition is approximately the same as the combined precision for traditional methods [27,28].

As a further test of the spectral method we have analyzed the broad melting curves of calf thymus, moose liver (*A. alces*) and salmon sperm DNAs. The dependence of $\Delta A_{282nm}/\Delta A_{260nm}$ on $f_{g\cdot c}$ for these DNAs are shown in Fig. 7. Despite considerable differences in their profiles, the fit to empirical Eqn. 4 (solid line) is excellent in all three cases.

Discussion

Results described satisfy two objectives: We have demonstrated the ability of the direct method to produce derivative melting curves on short homogeneous DNAs showing well resolved hyperfine detail. Also, we have derived a quantitative relationship between the ratio of melting curves obtained at 282 and 260 nm, and both instantaneous and total G + C composition. The estimated precision of this relationship appears to be better than ±3%; moreover, it is applicable to DNAs with base compositions beyond the usual range isolated in toto from a single species.

References

1 Yabuki, S., Wada, A
2 Gotoh, O., Husiml,
3 Ansevin, A.T. and E
4 Vizard, D.L. and Ar
5 Ansevin, A.T., Viza:
6 Lyubchenko, Yu.,
   (1976) Biopolymer;
7 Marmur, J. and Dot:
8 Church, R.B. and M
9 Paul, J. and Gilmou:
10 Massie, H. and Zimr
1 Hedgpeth, J., Good:
2 Blake, R.D., Massou
3 Riley, M., Maling, B
14 Römer, R., Riesner,
15 Guttman, T., Vitek,-
16 Felsenfeld, G. and S
17 Felsenfeld, G. and H
18 Fresco, J.R., Klotz.
   90
19 Fresco, J.R. (1963);
   p. 121, Academic P;
20 Coutts, S.M. (1971) .
21 Akiyama, C., Gotoh
22 Gasser, F. and Manc
23 Owen, R.J., Hill, L.:
24 Mandel, M., Igambi
   333—338.
25 Frank-Kamenetskii,
5 Tong, B.Y. and Leu.

Despite the many apparent advantages and disadvantages of the direct versus numerical methods for producing derivative melting curves, only one warrants serious attention: the ability to resolve subtransitional detail. The direct method appears to us at the present time to have a distinct advantage in principle. Resolution is limited only by the control of ΔT^* between samples. Moreover, instantaneous signal averaging is, more-or-less, an automatic feature of the double beam, ratio recording spectrophotometer; whereas smoothing steps of numerical methods incorporate fixed function constraints on absorbances. Smoothing procedures are probably adequate for simple profiles of predictable contour, such as produced by homopolynucleotide helices [29], repeating copolymers [30], and the very heterogeneous, broad melting eukaryotic DNAs [6,15]. However, it is very difficult to estimate the extent numerical procedures may lead to subtle distortions in the complex profiles of heteropolymers of unknown sequences, particularly those exhibiting over-lapping, closely spaced subtransitions.

Acknowledgements

References

1 Yabuki, S., Wada, A. and Uemura, K. (1969) J. Biochem. 65, 443—450
2 Gotoh, O., Husimi, Y., Yabuki, S. and Wada, A. (1976) Biopolymers 15, 655—670
3 Ansevin, A.T. and Brown, B. (1971) Biochemistry 10, 1133—1142
4 Vizard, D.L. and Ansevin, A.T. (1976) Biochemistry 15, 741—749
5 Ansevin, A.T., Vizard, D.L., Brown, B.W. and McConathy, J. (1976) Biopolymers 15, 153—174
6 Lyubchenko, Yu., Frank-Kamenetskii, M.D., Vologodskii, Yu., Lazurkin, S. and Gause, Jr., G.G. (1976) Biopolymers 15, 1019—1036
7 Marmur, J. and Doty, P.M. (1962) J. Mol. Biol. 5, 109—118
8 Church, R.B. and McCarty, B.J. (1968) Biochem. Genet. 2, 55—73
9 Paul, J. and Gilmour, R.S. (1968) J. Mol. Biol. 34, 305—316
10 Massie, H. and Zimm, B.H. (1969) Biopolymers 7, 475—493
11 Hedgpeth, J., Goodman, H.M. and Boyer, H.W. (1972) Proc. Natl. Acad. Sci. U.S. 69, 3448—3452
12 Blake, R.D., Massoulié, J. and Fresco, J.R. (1967) J. Mol. Biol. 30, 291—308
13 Riley, M., Maling, B. and Chamberlin, M.J. (1966) J. Mol. Biol. 20, 359—389
14 Römer, R., Riesner, D., Coutts, S.M. and Maass, G. (1970) Eur. J. Biochem. 15, 77—84
15 Guttman, T., Vitek, A. and Pivec, L. (1977) Nucleic Acid Res. 4, 285—297
16 Felsenfeld, G. and Sandeen, G. (1962) J. Mol. Biol. 5, 587—610
17 Felsenfeld, G. and Hirschman, S.Z. (1965) J. Mol. Biol. 13, 407—427
18 Fresco, J.R., Klotz, L.C. and Richards, E.G. (1963) Cold Spring Harbor Symp. Quant. Biol. 28, 83—90
19 Fresco, J.R. (1963) in Informational Macromolecules (Vogel, H.J., Bryson, V. and Lampen, J.D., eds.), p. 121, Academic Press, New York
20 Coutts, S.M. (1971) Biochim. Biophys. Acta 232, 94—106
21 Akiyama, C., Gotoh, O. and Wada, A. (1977) Biopolymers 16, 427—435
22 Gasser, F. and Mandel, M. (1968) J. Bacteriol. 96, 580—588
23 Owen, R.J., Hill, L.R. and Lepage, S.P. (1969) Biopolymers 7, 503—521
24 Mandel, M., Igambi, L., Bergendahl, J., Dodson, Jr., M.L. and Scheltgen, E. (1970) J. Bacteriol. 101, 333—338
25 Frank-Kamenetskii, M.D. (1971) Biopolymers 10, 2623—2624
26 Tong, B.Y. and Leung, M.L.C. (1977) Biopolymers 16, 1223—1231

27 Normore, W.M. and Brown, J.R. (1970) in Handbook of Biochemistry (Sober, H.A., ed.), 2nd edn., H-25—74, CRC, Cleveland
28 Shapiro, H.S. (1970) in Handbook of Biochemistry (Sober, H.A., ed.), 2nd edn., H-96—99, CRC, Cleveland
29 Blake, R.D. (1973) Biophys. Chem. 1, 24—34
30 Oliver, A.L., Wartell, R.M. and Ratliff, R.L. (1977) Biopolymers 16, 1115—1137

BBA 99131

ISOLATION A
DNA OF ALL(

GEORGE J. DIZI
Department of Mi
(Received July 18
(Revised manuscri

Summary

The mitocho
entrifugation a
mitochondri
confirmed by e
was homogenec
density analysis
1.702 g/cm^3, tl
daltons.

Introduction

The aquatic
system with w
development. M
genome [1,2]; t
ent is, howev
shown that D
differing in thei
nuclear DNA w
DNA. Examina
identification of
This study
purified A. ma
buoyant density
studies.

* Present addres
   Navarre, Minn
** To whom requ